

Istituto  
Nazionale  
Fisica  
Nucleare

Sezione SANITÀ  
Istituto Superiore di Sanità  
Viale Regina Elena 299  
I-00161 Roma, Italy

INFN-ISS 97/15  
November 1997

# Rare exclusive semileptonic $b \rightarrow s$ transitions in the Standard Model

D. Melikhov<sup>a</sup>, N. Nikitin<sup>a</sup> and S. Simula<sup>b</sup>

<sup>a</sup>Nuclear Physics Institute, Moscow State University  
Moscow, 119899, Russia

<sup>b</sup>Istituto Nazionale di Fisica Nucleare, Sezione Sanità  
Viale Regina Elena 299, I-00161 Roma, Italy

We study long-distance effects in rare exclusive semileptonic decays  $B \rightarrow (K, K^*) (\ell^+ \ell^-, \nu \bar{\nu})$  and analyze dilepton spectra and asymmetries within the framework of the Standard Model. The form factors, describing the meson transition amplitudes of the effective Hamiltonian are calculated within the lattice-constrained dispersion quark model: the form factors are given by dispersion representations through the wave functions of the initial and final mesons, and these wave functions are chosen such that the  $B \rightarrow K^*$  transition form factors agree with the lattice results at large  $q^2$ . We calculate branching ratios of semileptonic  $B \rightarrow K, K^*$  transition modes and study the sensitivity of observables to the long-distance contributions. The shape of the forward-backward asymmetry and the longitudinal lepton polarization asymmetry are found to be independent of the long-distance effects and mainly determined by the values of the Wilson coefficients in the Standard Model.

# Rare exclusive semileptonic $b \rightarrow s$ transitions in the Standard Model

D. Melikhov<sup>a</sup>, N. Nikitin<sup>a</sup> and S. Simula<sup>b</sup>

<sup>a</sup>*Nuclear Physics Institute, Moscow State University, Moscow, 119899, Russia*

<sup>b</sup>*Istituto Nazionale di Fisica Nucleare, Sezione Sanitá, Viale Regina Elena 299, I-00161 Roma, Italy*

We study long-distance effects in rare exclusive semileptonic decays  $B \rightarrow (K, K^*) (\ell^+ \ell^-, \nu \bar{\nu})$  and analyze dilepton spectra and asymmetries within the framework of the Standard Model. The form factors, describing the meson transition amplitudes of the effective Hamiltonian are calculated within the lattice-constrained dispersion quark model: the form factors are given by dispersion representations through the wave functions of the initial and final mesons, and these wave functions are chosen such that the  $B \rightarrow K^*$  transition form factors agree with the lattice results at large  $q^2$ . We calculate branching ratios of semileptonic  $B \rightarrow K, K^*$  transition modes and study the sensitivity of observables to the long-distance contributions. The shape of the forward-backward asymmetry and the longitudinal lepton polarization asymmetry are found to be independent of the long-distance effects and mainly determined by the values of the Wilson coefficients in the Standard Model.

PACS numbers: 13.20.He, 12.39.Ki, 12.39.Pn

## I. INTRODUCTION

The investigation of rare semileptonic decays of the  $B$  meson induced by the flavour-changing neutral current transitions  $b \rightarrow s$  represents an important test of the Standard Model (SM) and its possible extensions. Rare decays are forbidden at tree level and occur at the lowest order only through one-loop diagrams. This fact opens the possibility to probe at comparatively low energies the structure of the electroweak theory at large mass scales, thanks to the contributions of virtual particles in the loops. Moreover, rare  $b \rightarrow s$  transitions are expected to be sensitive to possible new interactions, like those provided, e.g., by supersymmetric theories, two Higgs-doublet, top-color and left-right models. These interactions govern the structure of the operators and the corresponding Wilson coefficients, which appear in the  $\Delta B = 1$  effective electroweak Hamiltonian describing the  $b \rightarrow s$  transitions at low energies.

A recent experimental observation of exclusive [1] and inclusive [2] radiative decays,  $B \rightarrow K^* \gamma$  and  $B \rightarrow X_s \gamma$ , have prompted a lot of theoretical investigation on rare semileptonic  $B$  decays. However, in the case of exclusive decays any reliable extraction of the perturbative (short-distance) effects encoded in the Wilson coefficients of the effective Hamiltonian [3–7] requires an accurate separation of the nonperturbative (long-distance) contributions, which therefore should be known with high accuracy. The theoretical investigation of these contributions encounters the problem of describing the hadron structure, which provides the main uncertainty in the predictions of exclusive rare decays.

In exclusive  $B \rightarrow K, K^*$  decays the long-distance effects in the meson transition amplitude of the effective Hamiltonian are encoded in the meson transition form factors of bilinear quark currents. Various theoretical frameworks have been applied to the description of meson transition form factors; among them we should mention constituent quark models [8–11], QCD sum rules [12–14], lattice QCD [15–17], approaches based on the heavy-quark symmetry [18] and analytical constraints [19].

Lattice QCD simulations, because of its most direct connection with QCD, are expected to provide the most reliable results. Although it is not possible to place the  $b$  quark directly on the lattice, a constrained extrapolation in the heavy quark mass [17] allows to determine reliably the form factors for  $B$  decays. A present limitation is that lattice calculations do not yet provide the form factors in the whole accessible kinematical decay region: the daughter light quark produced in  $b$  decay cannot move fast enough on the lattice and one is therefore limited to the region of not very large recoils. For obtaining form factors in the whole kinematical decay region one can use extrapolation procedures based on some parametrizations of the form factors. For instance, in [17] a simple lattice-constrained parametrization based on the constituent quark picture [9] and pole dominance is proposed. Anyway, a reliable knowledge of form factors in some region is already a substantial step forward, which provides firm constraints for the results of other approaches.

QCD sum rules give complementary information on the form factors as they can calculate the latter at not very large momentum transfers. However in practice various versions of the QCD sum rules give remarkably different predictions, being strongly dependent on the technical subtleties of the particular version. A recent analysis [20] disregards the three-point sum rules in favour of the light-cone sum rules. On the other hand, the light-cone sum rules involve more phenomenological inputs and the results turn out to be sensitive to the particular distribution amplitude of the light meson used in the evaluation of the sum rule and to the model adopted for the subtraction of the continuum (cf. [13] and [14]).

Constituent quark models (QM) have proved to be a fruitful phenomenological method for the description of heavy meson transitions. An attractive feature of the approaches based on the concept of constituent quarks is the suggestion of a simple physical picture of the decay process, based on the following phenomena responsible for the soft physics: i) the chiral symmetry breaking in the low-energy region generating the constituent quarks; ii) a strong peaking of the soft (nonperturbative) hadronic wave functions in terms of the relative constituent momenta with a width of the order of the confinement scale; and iii) the dominance of the contribution of the Fock state components with the minimal number of constituents, i.e.  $q\bar{q}$  component in mesons. An important shortcoming of the quark model predictions for the form factors is a strong dependence of the results on the QM parameters [11].

Thus we can see that none of the above-mentioned approaches can provide accurate form factors in the whole kinematically accessible region of  $B$  decays. In this situation a combination of the results of different approaches can be efficient for obtaining reliable predictions.

Our approach to the calculation of the  $B \rightarrow K, K^*$  transitions is based on the dispersion quark model [21,22]. The transition form factors are given by relativistic double spectral representations through the wave functions of the initial and final mesons both in the scattering and the decay regions. The form factors of the dispersion quark model develop the correct heavy-quark expansion at leading and next-to-leading  $1/m_Q$  orders in accordance with QCD for the transitions between heavy quarks [23,24]. For the heavy-to-light transition the form factors of the dispersion quark model satisfy the relations between the form factors of vector, axial-vector, and tensor currents valid at small recoil [25]. Thus the form factors of the dispersion quark model obey all known rigorous theoretical constraints. A possibility to calculate directly the form factors in all the decay region, avoiding in this way any extrapolation, is an important advantage of this formulation of the quark model. The main results of this work are as follows:

- We present a dispersion quark model calculation of the  $B \rightarrow K, K^*$  transition form factors in the whole kinematical range of  $q^2$ . Adopting the quark masses and the wave functions of the Godfrey-Isgur model [28] for the hadron spectrum with a switched-off one-gluon exchange (OGE) potential for taking into account only the impact of the confinement scale, we have found that the resulting form factors are in good agreement with the lattice simulations at large  $q^2$ . Thus we expect to provide reliable form factors in the whole decay region.

The dispersion quark model form factors for the  $B \rightarrow K^*$  transition agree favorably in the whole range of  $0 < q^2 < (M_B - M_K^*)^2$  with a lattice-constrained fit [17] based on the constituent quark picture [9] and an assumption on a single-pole behavior of the form factor  $A_1(q^2)$ . On the other hand the parametrizations based on heavy-quark symmetry (HQS) also give reasonable results if one assumes the leading-order expressions for the form factors and replaces the universal process-independent Isgur-Wise (IW) function with process-dependent form factors,  $\xi_{B \rightarrow K}$  and  $\xi_{B \rightarrow K^*}$ , related to the  $B \rightarrow K$  and  $B \rightarrow K^*$  transitions, respectively. The latter are found to differ strongly from each other and from the asymptotic IW function.

An important consequence is that both our QM calculations of the form factors and the lattice-constrained parametrization of Ref. [17] as well as the use of the heavy-quark symmetry relations between the form factors predict a quite similar behavior for the forward-backward and lepton polarization asymmetries.

- We derive formulas for the differential decay rates and asymmetries in exclusive rare semileptonic decays of heavy mesons for the case of massive leptons and taking into account a nonzero mass of the daughter quark produced in the rare  $b$  transition. For massless leptons and/or in the limit  $m_s \rightarrow 0$  our formulas reproduce known results.
- We present a detailed analysis of non-resonant decay rates and asymmetries in  $B \rightarrow (K, K^*) (\ell^+ \ell^-, \nu \bar{\nu})$  decays within the SM adopting our QM transition form factors. For comparison we also perform calculations with the lattice-constrained form factors of Ref. [17]. The decay rates evaluated in both models are found to be in agreement with each other, while the differential dilepton distributions are sensitive to subtle details of the  $q^2$ -dependence of the transition form factors. It is found that the lepton polarization asymmetry ( $P_L$ ) as well as the shape of the forward-backward asymmetry ( $A_{FB}$ ) are largely independent of the long-distance contributions and determined only by the values of the Wilson coefficients in the SM. Such features make both  $A_{FB}$  and  $P_L$  good candidates for testing the Standard Model and probing possible New Physics.

The paper is organized as follows. In Section II the SM operator basis, describing the  $b \rightarrow s\ell^+\ell^-$  and  $b \rightarrow s\nu\bar{\nu}$  transitions, is briefly presented. In Section III the meson transition form factors are considered. Section IV presents the differential rates, lepton spectra and lepton asymmetries for the rare  $B \rightarrow (K, K^*) (\ell^+ \ell^-, \nu \bar{\nu})$  decays including the case of massive leptons. Section V gives numerical analysis of the lepton spectra and lepton asymmetries in exclusive rare  $B$ -meson decays in the SM. Conclusion summarizes the results and gives an outlook.

## II. THE OPERATOR BASIS

The effective weak Hamiltonian, which describes the  $b \rightarrow s\ell^+\ell^-$  transition, has the following form [3]

$$\mathcal{H}_{eff} = \frac{G_F}{\sqrt{2}} V_{tb} V_{ts}^* \sum_i C_i(\mu) O_i(\mu), \quad (1)$$

where  $G_F$  is the universal Fermi constant, the quantities  $C_i(\mu)$  are the Wilson coefficients, obtained after integrating out the heavy particles, and the  $O_i$ 's are the basis operators; the sign of the Wilson coefficients  $C_i(\mu)$  is determined as in the work [3]:  $C_2(M_W) = -1$ . Within the SM, the operators providing the main contribution to rare decays are [4,5]

$$\begin{aligned} O_1 &= (\bar{s}_\alpha \gamma^\mu (1 - \gamma_5) b_\alpha) (\bar{c}_\beta \gamma_\mu (1 - \gamma_5) c_\beta), \\ O_2 &= (\bar{s}_\alpha \gamma^\mu (1 - \gamma_5) b_\beta) (\bar{c}_\beta \gamma_\mu (1 - \gamma_5) c_\alpha), \\ O_{7\gamma} &= \frac{e}{8\pi^2} \bar{s}_\alpha \sigma_{\mu\nu} [m_b(\mu)(1 + \gamma_5) + m_s(\mu)(1 - \gamma_5)] b_\alpha F^{\mu\nu}, \\ O_{9V} &= \frac{e^2}{8\pi^2} (\bar{s}_\alpha \gamma^\mu (1 - \gamma_5) b_\alpha) \bar{l} \gamma_\mu l, \\ O_{10A} &= \frac{e^2}{8\pi^2} (\bar{s}_\alpha \gamma^\mu (1 - \gamma_5) b_\alpha) \bar{l} \gamma_\mu \gamma_5 l, \end{aligned} \quad (2)$$

In Eq. (1) the renormalization scale  $\mu$  is usually chosen to be  $\mu \simeq m_b$  in order to avoid large logarithms in the matrix elements of the operators  $O_i$ . The Wilson coefficients  $C_i$  reflect the specific features of the theory at large mass scales; they are calculated at the scale  $\mu \simeq M_W$  and then evolved down to  $\mu \simeq m_b$  by the renormalization group equations. The analytic expressions for  $C_i(\mu)$  in the SM can be found, e.g., in [4]. In what follows, the values of the Wilson coefficients at the scale  $\mu \simeq m_b \simeq 5$  GeV are [3,4]:  $C_1(m_b) = 0.241$ ,  $C_2(m_b) = -1.1$ ,  $C_{7\gamma}(m_b) = 0.312$ ,  $C_{9V}(m_b) = -4.21$  and  $C_{10A}(m_b) = 4.64$ .

The four-quark operators  $O_1$  and  $O_2$  generate both short- and long-distance contributions to the effective weak Hamiltonian (1). Both contributions can be taken into account by replacing  $C_{9V}(m_b)$  with an effective coefficient  $C_{9V}^{eff}(m_b, q^2)$  given by [5]

$$C_{9V}^{eff}(m_b, q^2) = C_{9V}(m_b) + [3C_1(m_b) + C_2(m_b)] \cdot \left[ h\left(\frac{m_c}{m_b}, \frac{q^2}{m_b^2}\right) + \frac{3}{\alpha_{em}^2} \kappa \sum_{V_i=J/\psi, \psi', \dots} \frac{\pi \Gamma(V_i \rightarrow \ell\ell) M_{V_i}}{M_{V_i}^2 - q^2 - i M_{V_i} \Gamma_{V_i}} \right], \quad (3)$$

where  $q^2$  is the invariant mass squared of the lepton pair. The short-distance contributions are contained in the function  $h(m_c/m_b, q^2/m_b^2)$ , which describes the one-loop matrix element of the four-quark operators  $O_1$  and  $O_2$  (see, e.g., [4] for its explicit expression). The long-distance contribution, related to the formation of intermediate  $c\bar{c}$  bound states, is usually estimated by combining the factorization hypothesis and the Vector Meson Dominance assumption [5,6]; phenomenological analyses [6] suggest that in order to reproduce correctly the branching ratio  $\text{BR}(B \rightarrow J/\psi X \rightarrow \ell^+\ell^- X) = \text{BR}(B \rightarrow J/\psi X) \cdot \text{BR}(J/\psi \rightarrow \ell^+\ell^-)$  the fudge factor  $\kappa$ , which appears in Eq. (3) to correct phenomenologically for inadequacies of the factorization + VMD framework, should satisfy the approximate relation:  $\kappa [3C_1(m_b) + C_2(m_b)] \approx 1$ . To sum up, the effective weak Hamiltonian has the following structure (cf. [4,5,7])

$$\begin{aligned} \mathcal{H}_{eff}(b \rightarrow s\ell^+\ell^-) &= \frac{G_F}{\sqrt{2}} \frac{\alpha_{em}}{2\pi} V_{ts}^* V_{tb} \left[ -2 \frac{C_{7\gamma}(m_b)}{q^2} ((m_b + m_s)(\bar{s}i\sigma_{\mu\nu}q^\nu b) + (m_b - m_s)(\bar{s}i\sigma_{\mu\nu}q^\nu \gamma_5 b)) (\bar{l} \gamma^\mu l) \right. \\ &\quad \left. + C_{9V}^{eff}(m_b, q^2) (\bar{s} \gamma_\mu (1 - \gamma_5) b) (\bar{l} \gamma^\mu l) + C_{10A}(m_b) (\bar{s} \gamma_\mu (1 - \gamma_5) b) (\bar{l} \gamma^\mu \gamma_5 l) \right] \end{aligned} \quad (4)$$

$$\mathcal{H}_{eff}(b \rightarrow s\nu\bar{\nu}) = \frac{G_F}{\sqrt{2}} \frac{\alpha_{em}}{2\pi \sin^2 \theta_W} V_{tb} V_{ts}^* X(x_t) (\bar{s}_\alpha \gamma_\mu (1 - \gamma_5) b^\alpha) (\bar{\nu} \gamma^\mu (1 - \gamma_5) \nu) \quad (5)$$

where  $x_t = (m_t/M_W)^2$  and  $X(x_t)$  is given in [7]. At  $m_t = 176$  GeV one has  $X(x_t) = 2.02$ .

### III. MESON TRANSITION FORM FACTORS.

The long-distance contribution to  $B \rightarrow (K, K^*)$  decays is contained in the meson matrix elements of the bilinear quark currents of  $\mathcal{H}_{eff}$ , i.e. in the relativistic invariant transition form factors of the vector, axial-vector and tensor currents. In rare semileptonic decays there is another long-distance effect, known as the weak annihilation, which is caused by the Cabibbo-suppressed part of the four-fermion operators not included in the operator basis (1). However, the impact of this process in  $B \rightarrow (K, K^*)$  transitions is negligible [5]. The amplitudes of meson decays are induced by the quark transition  $b \rightarrow s$  through the vector  $V_\mu = \bar{s}\gamma_\mu b$ , axial-vector  $A_\mu = \bar{s}\gamma_\mu\gamma^5 b$ , tensor  $T_{\mu\nu} = \bar{s}\sigma_{\mu\nu} b$ , and pseudotensor  $T_{\mu\nu}^5 = \bar{q}\sigma_{\mu\nu}\gamma_5 b$  currents, with the following covariant structure [25]

$$\begin{aligned}
\langle P(M_2, p_2) | V_\mu(0) | P(M_1, p_1) \rangle &= f_+(q^2) P_\mu + f_-(q^2) q_\mu, \\
\langle V(M_2, p_2, \epsilon) | V_\mu(0) | P(M_1, p_1) \rangle &= 2g(q^2) \epsilon_{\mu\nu\alpha\beta} \epsilon^{*\nu} p_1^\alpha p_2^\beta, \\
\langle V(M_2, p_2, \epsilon) | A_\mu(0) | P(M_1, p_1) \rangle &= i\epsilon^{*\alpha} [f(q^2) g_{\mu\alpha} + a_+(q^2) p_{1\alpha} P_\mu + a_-(q^2) p_{1\alpha} q_\mu], \\
\langle P(M_2, p_2) | T_{\mu\nu}(0) | P(M_1, p_1) \rangle &= -2i s(q^2) (p_{1\mu} p_{2\nu} - p_{1\nu} p_{2\mu}), \\
\langle V(M_2, p_2, \epsilon) | T_{\mu\nu}(0) | P(M_1, p_1) \rangle &= i\epsilon^{*\alpha} [g_+(q^2) \epsilon_{\mu\nu\alpha\beta} P^\beta + g_-(q^2) \epsilon_{\mu\nu\alpha\beta} q^\beta + g_0(q^2) p_{1\alpha} \epsilon_{\mu\nu\beta\gamma} p_1^\beta p_2^\gamma], \\
\langle P(M_2, p_2) | T_{\mu\nu}^5(0) | P(M_1, p_1) \rangle &= s(q^2) \epsilon_{\mu\nu\alpha\beta} P^\alpha q^\beta, \\
\langle V(M_2, p_2, \epsilon) | T_{\mu\nu}^5(0) | P(M_1, p_1) \rangle &= g_+(q^2) (\epsilon_\nu^* P_\mu - \epsilon_\mu^* P_\nu) + g_-(q^2) (\epsilon_\nu^* q_\mu - \epsilon_\mu^* q_\nu) \\
&\quad + g_0(q^2) (p_{1\nu} \epsilon^* - p_{1\mu} p_{2\nu}) \tag{6}
\end{aligned}$$

where  $q = p_1 - p_2$ ,  $P = p_1 + p_2$ . We use the following notations:  $\gamma^5 = i\gamma^0\gamma^1\gamma^2\gamma^3$ ,  $\sigma_{\mu\nu} = \frac{i}{2}[\gamma_\mu, \gamma_\nu]$ ,  $\epsilon^{0123} = -1$ ,  $\gamma_5 \sigma_{\mu\nu} = -\frac{i}{2} \epsilon_{\mu\nu\alpha\beta} \sigma^{\alpha\beta}$ , and  $Sp(\gamma^5 \gamma^\mu \gamma^\nu \gamma^\alpha \gamma^\beta) = 4i\epsilon^{\mu\nu\alpha\beta}$ .

Another frequently used set of the form factors is connected with the set (6) as follows

$$\begin{aligned}
F_1(q^2) &= f_+(q^2), \\
F_0(q^2) &= f_+(q^2) + q^2 f_-(q^2)/(Pq), \\
F_T(q^2) &= -(M_1 + M_2) s(q^2), \\
V(q^2) &= (M_1 + M_2) g(q^2), \\
A_1(q^2) &= f(q^2)/(M_1 + M_2), \\
A_2(q^2) &= -(M_1 + M_2) a_+(q^2), \\
A_0(q^2) &= [q^2 a_-(q^2) + f(q^2) + (Pq) a_+(q^2)]/2M_2, \\
T_1(q^2) &= -g_+(q^2)/2, \\
T_2(q^2) &= -(g_+(q^2) + q^2 g_-(q^2))/(Pq)/2, \\
T_3(q^2) &= (M_1 + M_2)^2 [g_-(q^2)/(Pq) - h(q^2)/2]/2 \tag{7}
\end{aligned}$$

The relativistic invariant form factors encode the dynamical information about the decay process and should be considered within a nonperturbative approach. We investigate the meson form factors within a dispersion formulation of the relativistic constituent quark model (QM) model [21].

Let us consider the transition from the initial meson  $q(m_2)\bar{q}(m_3)$  with mass  $M_2$  to the final meson  $q(m_1)\bar{q}(m_3)$  with mass  $M_1$ , induced by the quark transition  $m_2 \rightarrow m_1$  through the current  $\bar{q}(m_1)J_{\mu(\nu)}q(m_2)$ . For the transition  $B_u \rightarrow (K, K^*)$  one has  $m_2 = m_b$ ,  $m_1 = m_s$  and  $m_3 = m_u$ . The  $CQ$  structure of the initial and final mesons is described by the vertices  $\Gamma_1$  and  $\Gamma_2$ , respectively. The initial  $B$ -meson vertex has the spinorial structure  $\Gamma_1 = i\gamma_5 G_1/\sqrt{N_c}$ , where  $N_c$  is the number of colours; the final meson vertex has the structure  $\Gamma_2 = i\gamma_5 G_2/\sqrt{N_c}$  for a pseudoscalar state and  $\Gamma_{2\mu} = [A\gamma_\mu + B(k_1 - k_3)_\mu] G_2/\sqrt{N_c}$ , with  $A = -1$  and  $B = 1/(\sqrt{s_2} + m_1 + m_3)$  for an  $S$ -wave vector meson. At  $q^2 < 0$  the spectral representations of the form factors have the form [21]

$$f_i(q^2) = \frac{1}{16\pi^2} \int_{(m_1+m_3)^2}^{\infty} ds_2 \varphi_2(s_2) \int_{s_1^-(s_2, q^2)}^{s_1^+(s_2, q^2)} ds_1 \varphi_1(s_1) \frac{\tilde{f}_i(s_1, s_2, q^2)}{\lambda^{1/2}(s_1, s_2, q^2)}, \tag{8}$$

where the wave function  $\varphi_i(s_i) = G_i(s_i)/(s_i - M_i^2)$  and

$$s_1^\pm(s_2, q^2) = \frac{s_2(m_1^2 + m_2^2 - q^2) + q^2(m_1^2 + m_3^2) - (m_1^2 - m_2^2)(m_1^2 - m_3^2)}{2m_1^2} \pm \frac{\lambda^{1/2}(s_2, m_3^2, m_1^2) \lambda^{1/2}(q^2, m_1^2, m_2^2)}{2m_1^2}$$

and  $\lambda(s_1, s_2, s_3) = (s_1 + s_2 - s_3)^2 - 4s_1s_2$  is the triangle function.

The Eq. (8) accounts for only two-particle singularities in the Feynman graphs. For ground-state pseudoscalar and vector mesons built up of constituent quarks with the masses  $m_q$  and  $m_{\bar{q}}$ , the function  $\varphi(s)$  can be written as

$$\varphi(s) = \frac{\pi}{\sqrt{2}} \frac{\sqrt{s^2 - (m_q^2 - m_{\bar{q}}^2)^2}}{\sqrt{s - (m_q - m_{\bar{q}})^2}} \frac{w(k^2)}{s^{3/4}}, \quad (9)$$

where  $k = \lambda^{1/2}(s, m_q^2, m_{\bar{q}}^2)/2\sqrt{s}$  and  $w(k^2)$  is the ground-state  $S$ -wave radial wave function, normalized as  $\int_0^\infty dk k^2 |w(k^2)|^2 = 1$ .

The unsubtracted double spectral densities  $\tilde{f}_i(s_1, s_2, q^2)$  of the form factors read [22]:

$$\tilde{s} = 2[m_1\alpha_2 + m_2\alpha_1 + m_3(1 - \alpha_1 - \alpha_2)], \quad (10)$$

$$\tilde{f}_+ + \tilde{f}_- \equiv \tilde{f}_1 = 2m_1\tilde{s} + 4\alpha_2[s_2 - (m_1 - m_3)^2] - 2m_3\tilde{s}, \quad (11)$$

$$\tilde{f}_+ - \tilde{f}_- \equiv \tilde{f}_2 = 2m_2\tilde{s} + 4\alpha_1[s_1 - (m_2 - m_3)^2] - 2m_3\tilde{s}, \quad (12)$$

$$\tilde{g} = -A\tilde{s} - 4B\beta, \quad (13)$$

$$\tilde{g}_+ + \tilde{g}_- = A\tilde{f}_1 - 8\beta + 8B(m_1 + m_3)\beta, \quad (14)$$

$$\tilde{g}_+ - \tilde{g}_- = A\tilde{f}_2 + 8B(m_2 - m_3)\beta, \quad (15)$$

$$\tilde{a}_{+D} - \tilde{a}_{-D} = -2\tilde{s} + 4BC_2\alpha_1 + \alpha_{12}C_0, \quad (16)$$

$$\tilde{a}_{+D} + \tilde{a}_{-D} = -4A(2m_3 + BC_1)\alpha_1 + \alpha_{11}C_0, \quad (17)$$

$$\tilde{f}_D = -4A[m_1m_2m_3 + \frac{m_2}{2}(s_2 - m_1^2 - m_3^2) + \frac{m_1}{2}(s_1 - m_2^2 - m_3^2) - \frac{m_3}{2}(s_3 - m_1^2 - m_2^2)] + C_0\beta, \quad (18)$$

$$\tilde{g}_{0D} = -8A\alpha_{12} - 8B[-m_3\alpha_1 + (m_3 - m_2)\alpha_{11} + (m_3 + m_1)\alpha_{12}], \quad (19)$$

where

$$\alpha_1 = [(s_1 + s_2 - s_3)(s_2 - m_1^2 + m_3^2) - 2s_2(s_1 - m_2^2 + m_3^2)]/\lambda(s_1, s_2, s_3), \quad (20)$$

$$\alpha_2 = [(s_1 + s_2 - s_3)(s_1 - m_2^2 + m_3^2) - 2s_1(s_2 - m_1^2 + m_3^2)]/\lambda(s_1, s_2, s_3), \quad (21)$$

$$\beta = \frac{1}{4} [2m_3^2 - \alpha_1(s_1 - m_2^2 + m_3^2) - \alpha_2(s_2 - m_1^2 + m_3^2)], \quad (22)$$

$$\alpha_{11} = \alpha_1^2 + 4\beta s_2/\lambda(s_1, s_2, s_3), \quad \alpha_{12} = \alpha_1\alpha_2 - 2\beta(s_1 + s_2 - s_3)/\lambda(s_1, s_2, s_3), \quad (23)$$

$$C_0 = -8A(m_2 - m_3) + 4BC_3, \quad C_1 = s_2 - (m_1 + m_3)^2, \quad (24)$$

$$C_2 = s_1 - (m_2 - m_3)^2, \quad C_3 = s_3 - (m_1 + m_2)^2 - C_1 - C_2.$$

We label with a subscript 'D' the double spectral densities of the form factors which require subtractions. The subtraction procedure has been fixed by matching the  $1/m_Q$  expansion of the form factors in the quark model to the corresponding expansion in QCD in leading and next-to-leading orders for the case of a meson transition caused by heavy-to-heavy quark transition [22].

The double spectral densities with properly defined subtraction terms read

$$\tilde{f} = \tilde{f}_D + [(M_1^2 - s_1) + (M_2^2 - s_2)]\tilde{g}, \quad (25)$$

$$\tilde{a}_+ = \tilde{a}_{+D} + \frac{\sqrt{s_1} + \sqrt{s_2}}{(\sqrt{s_1} + \sqrt{s_2})^2 - s_3} \left( \frac{M_1^2 - s_1}{\sqrt{s_1}} + \frac{M_2^2 - s_2}{\sqrt{s_2}} \right) \frac{\tilde{g}}{2}, \quad (26)$$

$$\tilde{a}_- = \tilde{a}_{-D} + \frac{\sqrt{s_2} - \sqrt{s_1}}{(\sqrt{s_1} + \sqrt{s_2})^2 - s_3} \left( \frac{M_1^2 - s_1}{\sqrt{s_1}} + \frac{M_2^2 - s_2}{\sqrt{s_2}} \right) \frac{\tilde{g}}{2}, \quad (27)$$

$$\tilde{g}_0 = \tilde{g}_{0D} + \frac{1}{(\sqrt{s_1} + \sqrt{s_2})^2 - s_3} \left( \frac{M_1^2 - s_1}{\sqrt{s_1}} + \frac{M_2^2 - s_2}{\sqrt{s_2}} \right) \tilde{g}. \quad (28)$$

The structure of the HQ expansion in LO and NLO  $1/m_Q$  orders of the form factors given by the Eq. (8) with the spectral densities (10-refg0) agrees with the corresponding structure of the HQ expansion in QCD [24], provided that the functions  $\varphi(s_i)$  are localized near the  $q\bar{q}$  threshold with a width of the order  $\Lambda_{QCD}$  [22]. Moreover, for the case of meson decays induced by a heavy-to-light quark transition the dispersion formulation provides the form factors which satisfy the leading-order relations between the form factors of the vector and tensor currents near zero recoil given in [25].

As the analytical continuation to the time-like region  $q^2 > 0$  is performed, in addition to the normal contribution which is just the expression (8) taken at  $q^2 > 0$ , the anomalous contribution, described explicitly in [21]

emerges. The normal contribution dominates the form factors at small  $q^2$  and vanishes when  $q^2 = (m_2 - m_1)^2$ , while the anomalous contribution is negligible at small  $q^2 > 0$  and steeply rises as  $q^2 \rightarrow (m_2 - m_1)^2$ .

Notice that since the dispersion quark model is based on taking into account only two-particle  $q\bar{q}$  intermediate states in the amplitude of the interaction of the  $q\bar{q}$  constituent quark pair with the external field it is conceptually close to the light-cone quark model LCQM [8]. In particular, the form factors of the LCQM [8] can be rewritten at  $q^2 < 0$  as double spectral representations similar to the dispersion model. One finds that at  $q^2 < 0$  the form factors which are given by the unsubtracted spectral representations in the dispersion formulation are the same as in the LCQM. At the same time, the LCQM form factors  $f$ ,  $a_1$ ,  $a_2$ , and  $h$  are different from the dispersion quark model form factors and do not develop a correct heavy quark expansion in the next-to-leading  $1/m_Q$  order.

For evaluating the form factors we need to specify the quark model parameters such as the constituent quark masses and the wave functions. In Ref. [11] we have run calculations of the mesonic form factors (8) adopting different QMs for the radial wave function  $w(k^2)$  appearing in Eq. (9), in particular: a simple Gaussian ansatz of the ISGW2 model [26] and the variational solution [27] of the effective  $q\bar{q}$  semi-relativistic Hamiltonian of Godfrey and Isgur (GI) [28]. These two models differ both in the shape of the radial wave function, particularly at high momenta  $k$ , and in the values of the quark masses (see Ref. [11]). The results of our calculations have shown that the mesonic form factors (8) are sensitive both to the high-momentum tail of the meson wave function and to the values adopted for the quark masses (see also Refs. [29,30]).

In order to obtain more reliable predictions for the form factors, we require the QM parameters to be adjusted in such a way that the calculated form factors at large  $q^2$  are compatible with the lattice results [15,16]. We have found that the best agreement with the lattice data at large  $q^2$  is obtained for the quark masses and wave functions of the GI model with a switched-off one-gluon exchange (GI-OGE). The constituent quark masses and the average momenta squared characterizing the GI-OGE model are given in Table I. Table II presents simple fits to the calculated form factors.

Fig. 1 shows the GI-OGE form factors versus the available lattice data for  $B \rightarrow K^*$  [15,16]. For comparison, we also present the form factors obtained within the ISGW2 exponential ansatz for the soft meson wave functions [11].

A good agreement of our QM predictions obtained with the GI-OGE wave functions with the results of lattice simulations is not surprising: the strong long-distance physics is dominated by the confinement mechanism, and therefore it seems quite natural, that soft wave functions which take into account the effects of the confinement scale provide the form factors in agreement with the lattice QCD results.

TABLE I. Constituent quark masses (in  $GeV$ ) and the average momentum squared (in  $GeV^2$ ).

Ref.	$m_u$	$m_s$	$m_c$	$m_b$	$\langle k^2 \rangle_K$	$\langle k^2 \rangle_{K^*}$	$\langle k^2 \rangle_{B_u}$
GI-OGE [27]	0.22	0.42	1.65	5.0	0.17	0.17	0.26

TABLE II. Parameters of the fit  $f_i(q^2) = f_i(0)/[1 - \sigma_1 q^2 + \sigma_2 q^4]$  to the  $B \rightarrow (K, K^*)$  transition form factors in the GI-OGE model.

Decay	$B \rightarrow K$			$B \rightarrow K^*$						
	$f_+(0)$	$f_-(0)$	$s(0)$	$g(0)$	$f(0)$	$a_+(0)$	$a_-(0)$	$h(0)$	$g_+(0)$	$g_-(0)$
Ref.	$f_+(0)$	$f_-(0)$	$s(0)$	$g(0)$	$f(0)$	$a_+(0)$	$a_-(0)$	$h(0)$	$g_+(0)$	$g_-(0)$
	$\sigma_1$	$\sigma_1$	$\sigma_1$	$\sigma_1$	$\sigma_1$	$\sigma_1$	$\sigma_1$	$\sigma_1$	$\sigma_1$	$\sigma_1$
	$\sigma_2$	$\sigma_2$	$\sigma_2$	$\sigma_2$	$\sigma_2$	$\sigma_2$	$\sigma_2$	$\sigma_2$	$\sigma_2$	$\sigma_2$
GI-OGE	0.33	-0.27	0.057	0.063	2.01	-0.0454	0.053	0.0056	-0.3540	0.313
	0.0519	0.0524	0.0517	0.0523	0.0212	0.039	0.044	0.0657	0.0523	0.053
	0.00065	0.00066	0.00064	0.00066	0.00009	0.00004	0.00023	0.0010	0.0007	0.00067

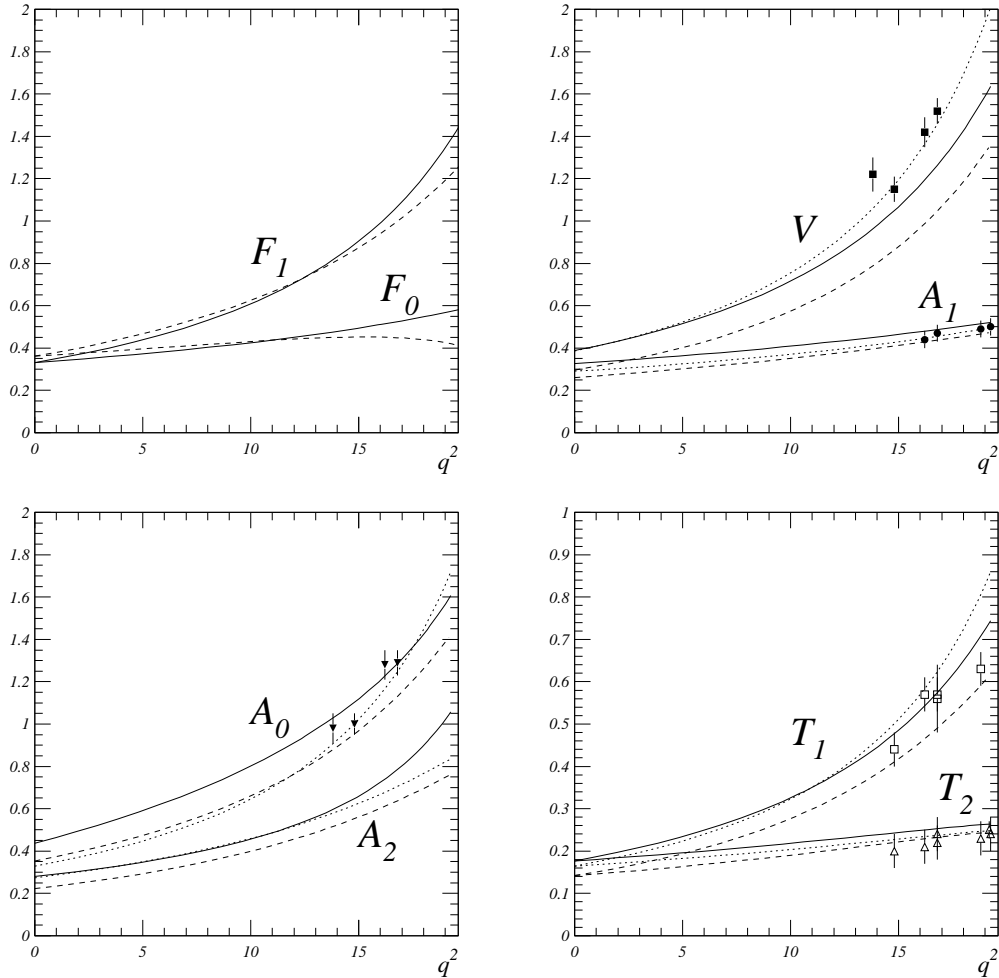


FIG. 1. Form factors for the  $B \rightarrow K, K^*$  transition vs the lattice data: solid - GI-OGE, dashed - ISGW2 models, dotted - lattice-constrained parametrization [17].

Recently, a lattice-constrained parametrization for the  $B \rightarrow K^*$  form factors has been developed in the whole range of accessible values of  $q^2$  [16]. It is based on the Stech parametrization of the form factors obtained within the constituent quark picture, HQS scaling relations near  $q^2 = q_{max}^2$  and a single-pole behavior of  $A_1$  suggested by  $m_Q$ -scaling relations at  $q^2 = 0$  from the LCSR in the HQ limit. Parameters of the single-pole fit to the form factor  $A_1(0) = 0.29^{+0.04}_{-0.03}$  and  $M_1 = 6.8^{+0.7}_{-0.4} \text{ GeV}$  are found from the least- $\chi^2$  fit to the lattice QCD simulation in a limited region at high values of  $q^2$ . Such a parametrization, though still phenomenological, is also consistent with the dispersive bounds of Ref. [19] and therefore obeys all known theoretical constraints. It should be taken into account however that the lattice-constrained parametrization is an approximation: in particular, it suggests the relation  $T_1(q^2) = (1 - q^2/Pq)T_2(q^2)$  which can be also translated into  $g_+(q^2) = -g_-(q^2)$ . In dynamical calculation within QMs or LCSR these relations are fulfilled within 10% accuracy but are never found to be exact. Nevertheless, approximate Stech's relations combined with a monopole fit to  $A_1$  exhibit surprisingly good agreement with the lattice points at large  $q^2$  (see Fig. 1).

The form factor  $A_1$  calculated in our approach for the GI-OGE model wave functions is found to have a behavior very close to the single-pole function with the parameters  $A_1(0) = 0.326$  and  $M_1 = 6.86 \text{ GeV}$  in agreement with an assumption of Ref. [17]. The results on most of the form factors are within 5% agreement with the parametrizations [17] except for the form factor  $V$  which turns out to be at zero recoil some 15% smaller in our calculations.

Table III compares predictions on the form factors from various approaches. One can see that our results agree with those of the LCSR of Ref. [14]. The form factors of another version of the LCSR [13] have different behavior which disagrees also with the lattice results at large  $q^2$ : namely, at  $q^2 \simeq 16 \text{ GeV}^2$  the form factors  $T_1, T_2$ , and  $A_1$  turn out to be considerably larger than the lattice points, and the form factor  $A_0$  to be too small. The form factors  $T_2$  and  $A_1$  in the 3ptSR approach [12] are decreasing with  $q^2$  in contradiction with the results of other approaches and lattice simulations.

Let us notice, that an approximate relation  $g_+ = -g_-$  found to describe well the lattice points at large  $q^2$

and extended in [17] to the whole kinematically accessible region, might signal that relations motivated by the heavy-quark symmetry also work with a reasonable accuracy in the  $B \rightarrow K, K^*$  case. In fact, the HQ expansion of the form factors  $g_+$  and  $g_-$  gives  $g_+ = \frac{M_1+M_2}{2\sqrt{M_1M_2}} \xi_{IW}(\omega)[1+O(1/m_Q)]$  and  $g_- = -\frac{M_1-M_2}{2\sqrt{M_1M_2}} \xi_{IW}(\omega)[1+O(1/m_Q)]$ . An approximate relation  $g_+ = -g_-$  can be obtained from this expansion in the limit  $M_K^* \ll M_B$  only if the generically different combinations  $\xi_{IW}(\omega)[1+O(1/m_Q)]$  in  $g_+$  and  $g_-$  evolve in this limit to the same function  $\xi_{B \rightarrow K^*}$  which however goes far from the Isgur-Wise function. Let us assume the leading-order IW relations for the form factors with the IW function replaced by the function  $\xi_{B \rightarrow K}$  and  $\xi_{B \rightarrow K^*}$  for  $B \rightarrow K$  and  $B \rightarrow K^*$  transitions, respectively. The process-dependent functions  $\xi_{B \rightarrow K, K^*}$  determined from the GI-OGE QM results for  $T_1$  and  $F_1$  through the relations

$$\xi_{B \rightarrow K^*} = \frac{4\sqrt{M_B M_K^*}}{M_B + M_K^*} T_1, \quad \xi_{B \rightarrow K} = \frac{2\sqrt{M_B M_K^*}}{M_B + M_K^*} F_1 \quad (29)$$

are shown in Fig. 2. The deviations for other form factors of  $B \rightarrow K^*$  transition found through the LO HQS relations with  $\xi_{B \rightarrow K^*}$  from the lattice-constrained parametrizations can be as much as 20%.

Summing up, the dispersion quark model calculates the form factors in the whole kinematically accessible decay region. The form factors of the dispersion quark model have the following properties: they develop a correct HQ expansion in the leading and next-to-leading  $1/m_Q$  orders in agreement with QCD in heavy-to-heavy transitions provided the soft wave function is concentrated in the region of the confinement scale; for the case of heavy-to-light transition they have the correct scaling properties at small recoil and obey the LO  $1/m_Q$  relations between the form factors of  $V, A$ , and  $T$  currents [25]; and numerically they agree with the lattice results at large  $q^2$  for the  $B \rightarrow K^*$  transitions. Thus we expect the dispersion quark model form factors to be reliable in the whole kinematically accessible region.

In the next sections we use the QM form factors evaluated with the GI-OGE wave functions and the lattice-constrained parametrizations of Ref. [17] for analyzing the decay rates and asymmetries in rare  $B$  decays.

TABLE III. Comparison of the results of different approaches on the form factors  $T_1, T_2, A_1$  and  $A_0$  at  $q^2 = 0$  and  $q^2 = 16.2 \text{ GeV}^2$ .

Ref.	$T_1$		$T_2$		$A_1$		$A_0$	
	$q^2 = 0$	$q^2 = 16.2 \text{ GeV}^2$	$q^2 = 16.2 \text{ GeV}^2$	$q^2 = 0$	$q^2 = 16.2 \text{ GeV}^2$	$q^2 = 0$	$q^2 = 16.2 \text{ GeV}^2$	
LCQM [8]	0.155	0.53	0.26	0.26	0.45	0.32	—	
3ptSR [12]	$0.19 \pm 0.03$	$0.5 \pm 0.05$	$0.13 \pm 0.03$	$0.37 \pm 0.03$	$0.23 \pm 0.03$	$0.3 \pm 0.03$	$1.0 \pm 0.05$	
LCSR [13]	0.18	0.84	0.35	0.36	0.65	0.27	0.64	
LCSR+Lat [14]	$0.15 \pm 0.04$	0.54	0.22	—	—	—	—	
Lat+ [17]	$0.16_{-0.01}^{+0.02}$	$0.57 \pm 0.04$	$0.21 \pm 0.04$	0.29	$0.44 \pm 0.04$	0.33	$1.28 \pm 0.07$	
GI-OGE	0.177	0.53	0.248	0.33	0.44	0.44	1.20	
ISGW2	0.142	0.46	0.23	0.26	0.42	0.35	1.08	

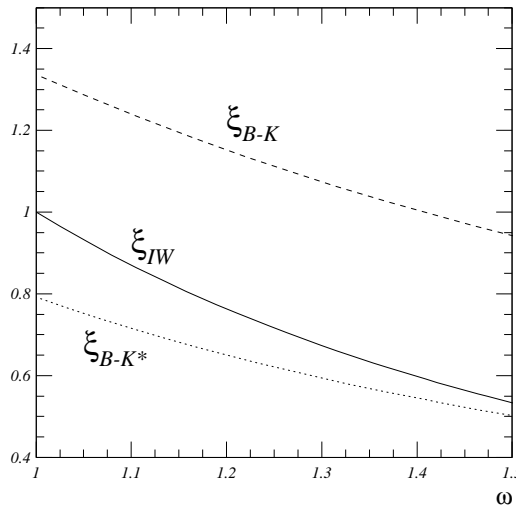


FIG. 2. The Isgur-Wise function  $\xi$  (solid) [22,30], and the form factor  $\xi_{B \rightarrow K}$  (dotted) and  $\xi_{B \rightarrow K^*}$  (dashed) calculated via Eq. (29).

#### IV. DIFFERENTIAL DECAY RATES AND LEPTON ASYMMETRIES

In this Section we present formulas for the differential decay rates, forward-backward asymmetries and lepton polarization asymmetries obtained for both  $m_s \neq 0$  and  $m_s \neq 0$  for the transition induced by the effective Hamiltonian Eq. (4) in the case  $B \rightarrow (K, K^*)(\ell^+ \ell^-)$  and by Eq. (5) in the case  $B \rightarrow (K, K^*)(\nu \bar{\nu})$ .

Our formulas for the differential decay rates and forward-backward asymmetry coincide with the corresponding formulas of Ref. [31] and reproduce the formulas of Refs. [10,13] in the case  $m_s = 0$  and  $m_l \neq 0$  and those of Ref. [12] in the case  $m_s = 0, m_l = 0$ . For lepton polarization asymmetries our expressions in the limit  $m_s = 0$  coincide with the results of [10,13].

Introducing the dimensionless kinematical variables  $\hat{s} \equiv q^2/M_B^2$  and  $\hat{t} \equiv (P_B - p_{l+})^2/M_B^2$ , the double differential decay width for the rare decay  $B \rightarrow K \ell^+ \ell^-$  can be cast into the form

$$\frac{d^2\Gamma(B \rightarrow K \ell^+ \ell^-)}{d\hat{s} d\hat{t}} = \frac{G_F^2 M_B^5 |V_{ts}^* V_{tb}|^2 \alpha_{em}^2}{256\pi^5} \left[ -\hat{\Pi} \beta_P + 2\hat{m} \delta_P \right], \quad (30)$$

where

$$\begin{aligned} \beta_P &= \left| C_{9V}^{eff}(m_b, q^2) f_+(q^2) + 2(m_b + m_s) C_{7\gamma}(m_b) s(q^2) \right|^2 + \left| C_{10A}(m_b) f_+(q^2) \right|^2, \\ \hat{\Pi} &= (\hat{t} - 1)(\hat{t} - \hat{r}) + \hat{s}\hat{t} + \hat{m}(1 + \hat{r} + \hat{m} - \hat{s} - 2\hat{t}), \\ \delta_P &= |C_{10A}|^2 \left\{ \left( 1 + \hat{r} - \frac{\hat{s}}{2} \right) |f_+(q^2)|^2 + (1 - \hat{r}) \text{Re}[f_+(q^2) f_-^*(q^2)] + \frac{\hat{s}}{2} |f_-(q^2)|^2 \right\} \end{aligned} \quad (31)$$

with  $\hat{r} \equiv (M_K/M_B)^2$  and  $\hat{m} \equiv (m_\ell/M_B)^2$ . After integrating over  $\hat{t}$  from  $\hat{t}_{min} = [1 + \hat{r} + 2\hat{m} - \hat{s} - \sqrt{1 - 4\hat{m}/\hat{s}}\lambda^{1/2}(1, \hat{s}, \hat{r})]/2$  to  $\hat{t}_{max} = [1 + \hat{r} + 2\hat{m} - \hat{s} + \sqrt{1 - 4\hat{m}/\hat{s}}\lambda^{1/2}(1, \hat{s}, \hat{r})]/2$ , where  $\lambda(1, \hat{s}, \hat{r}) = 1 + \hat{r}^2 + \hat{s}^2 - 2\hat{r} - 2\hat{s} - 2\hat{r}\hat{s}$ , one obtains the invariant dilepton mass distribution

$$\frac{d\Gamma(B \rightarrow K \ell^+ \ell^-)}{d\hat{s}} = \frac{G_F^2 M_B^5 |V_{ts}^* V_{tb}|^2 \alpha_{em}^2}{1536\pi^5} \sqrt{1 - 4\hat{m}/\hat{s}} \lambda^{1/2}(1, \hat{s}, \hat{r}) \left[ \left( 1 + \frac{2\hat{m}}{\hat{s}} \right) \lambda(1, \hat{s}, \hat{r}) \beta_P + 12\hat{m} \delta_P \right], \quad (32)$$

In the case of the decay  $B \rightarrow K^* \ell^+ \ell^-$  one has

$$\frac{d^2\Gamma(B \rightarrow K^* \ell^+ \ell^-)}{d\hat{s} d\hat{t}} = \frac{G_F^2 M_B^5 |V_{ts}^* V_{tb}|^2 \alpha_{em}^2}{512\pi^5} \left[ \beta_V^{(1)} + \beta_V^{(2)} + 4\hat{m} \delta_V \right], \quad (33)$$

with

$$\begin{aligned} \beta_V^{(1)} &= \left[ (\hat{s} + 2\hat{m}) \lambda(1, \hat{s}, \hat{r}) + 2\hat{s}\hat{\Pi} \right] |G(q^2)|^2 + \left[ \hat{s} + 2\hat{m} - \frac{\hat{\Pi}}{2\hat{r}} \right] |F(q^2)|^2 \\ &\quad - \frac{\lambda^2(1, \hat{s}, \hat{r})}{2\hat{r}} \hat{\Pi} |H_+(q^2)|^2 + \frac{\hat{s} - 1 + \hat{r}}{\hat{r}} \hat{\Pi} |R(q^2)|^2, \\ \beta_V^{(2)} &= 2\hat{s}[2\hat{t} + \hat{s} - \hat{r} - 1 - 2\hat{m}] R_1(q^2) \\ |G(q^2)|^2 &= \left| C_{9V}^{eff}(m_b, q^2) M_B g(q^2) - \frac{2C_{7\gamma}(m_b)}{\hat{s}} \frac{m_b + m_s}{M_B} g_+(q^2) \right|^2 + |C_{10A}(m_b) M_B g(q^2)|^2, \\ |F(q^2)|^2 &= \left| C_{9V}^{eff}(m_b, q^2) \frac{f(q^2)}{M_B} - \frac{2C_{7\gamma}(m_b)}{\hat{s}} \frac{m_b - m_s}{M_B} (1 - \hat{r}) B_0(q^2) \right|^2 + \left| C_{10A}(m_b) \frac{f(q^2)}{M_B} \right|^2, \\ |H_+(q^2)|^2 &= \left| C_{9V}^{eff}(m_b, q^2) M_B a_+(q^2) - \frac{2C_{7\gamma}(m_b)}{\hat{s}} \frac{m_b - m_s}{M_B} B_+(q^2) \right|^2 + |C_{10A}(m_b) M_B a_+(q^2)|^2, \\ R(q^2) &= \text{Re} \left\{ \left[ C_{9V}^{eff}(m_b, q^2) \frac{f(q^2)}{M_B} - \frac{2C_{7\gamma}(m_b)}{\hat{s}} \frac{m_b - m_s}{M_B} (1 - \hat{r}) B_0(q^2) \right] \left[ C_{9V}^{eff}(m_b, q^2) M_B a_+(q^2) \right. \right. \\ &\quad \left. \left. - \frac{2C_{7\gamma}(m_b)}{\hat{s}} \frac{m_b - m_s}{M_B} B_+(q^2) \right]^* \right\} + |C_{10A}(m_b)|^2 \text{Re}[a_+(q^2) f^*(q^2)], \\ R_1(q^2) &= \text{Re} \left\{ \left[ C_{9V}^{eff}(m_b, q^2) M_B g(q^2) - \frac{2C_{7\gamma}(m_b)}{\hat{s}} \frac{m_b + m_s}{M_B} g_+(q^2) \right] \left[ C_{10A}(m_b) \frac{f(q^2)}{M_B} \right]^* \right\} \\ &\quad + \text{Re} \left\{ \left[ C_{9V}^{eff}(m_b, q^2) \frac{f(q^2)}{M_B} - \frac{2C_{7\gamma}(m_b)}{\hat{s}} \frac{m_b - m_s}{M_B} (1 - \hat{r}) B_0(q^2) \right] \left[ C_{10A}(m_b) M_B g(q^2) \right]^* \right\}, \end{aligned}$$

$$\begin{aligned}
B_0(q^2) &= g_+(q^2) + g_-(q^2) \frac{\hat{s}}{1-\hat{r}}, \\
B_+(q^2) &= -\hat{s} M_B^2 \frac{h(q^2)}{2} - g_+(q^2), \\
\delta_V &= \frac{|C_{10A}|^2}{2} \lambda(1, \hat{s}, \hat{r}) \left\{ -2|g(q^2)M_B|^2 - \frac{3}{\lambda(1, \hat{s}, \hat{r})} \left| \frac{f(q^2)}{M_B} \right|^2 + \frac{2(1+k)-\hat{s}}{4\hat{r}} |a_+(q^2)M_B|^2 \right. \\
&\quad \left. + \frac{\hat{s}}{4\hat{r}} |a_-(q^2)M_B|^2 + \frac{1}{2\hat{r}} \text{Re}[f(q^2)a_+^*(q^2) + f(q^2)a_-^*(q^2)] + \frac{1-\hat{r}}{2\hat{r}} \text{Re}[M_B a_+(q^2) M_B a_-^*(q^2)] \right\}. \quad (34)
\end{aligned}$$

where now  $\hat{r} \equiv (M_{K^*}/M_B)^2$ . After integrating over the variable  $\hat{t}$  we find

$$\frac{d\Gamma(B \rightarrow K^* \ell^+ \ell^-)}{d\hat{s}} = \frac{G_F^2 M_B^5 |V_{ts}^* V_{tb}|^2 \alpha_{em}^2}{1536\pi^5} \sqrt{1-4\hat{m}/\hat{s}} \lambda^{1/2}(1, \hat{s}, \hat{r}) \left[ \left( 1 + \frac{2\hat{m}}{\hat{s}} \right) \beta_V + 12\hat{m}\delta_V \right], \quad (35)$$

where

$$\begin{aligned}
\beta_V &= 2\lambda(1, \hat{s}, \hat{r})\hat{s}|G(q^2)|^2 + \left[ 2\hat{s} + \frac{(1-\hat{r}-\hat{s})^2}{4\hat{r}} \right] |F(q^2)|^2 + \frac{\lambda^2(1, \hat{s}, \hat{r})}{4\hat{r}} |H_+(q^2)|^2 \\
&\quad - \frac{\lambda(1, \hat{s}, \hat{r})}{2\hat{r}} (\hat{s} - 1 + \hat{r}) R(q^2). \quad (36)
\end{aligned}$$

The effective Hamiltonian for the  $B \rightarrow (K, K^*)(\nu\bar{\nu})$  transition (5) may be obtained from the corresponding Hamiltonian for the  $B \rightarrow (K, K^*)(\ell^+ \ell^-)$  transition (4) by the following replacements:

$$\hat{m} \rightarrow 0, C_{7\gamma} \rightarrow 0, C_{9V}^{eff} \rightarrow \frac{X(x_t)}{\sin^2(\theta_W)}, C_{10A} \rightarrow -\frac{X(x_t)}{\sin^2(\theta_W)}. \quad (37)$$

Hence, expressions for the decay rates in  $B \rightarrow (K, K^*)(\nu\bar{\nu})$  can be obtained from the corresponding formulas for  $B \rightarrow (K, K^*)(\ell^+ \ell^-)$  by the replacement (37).

For the decays  $B \rightarrow K^* \ell^+ \ell^-$  a very interesting quantity is the forward-backward (FB) charge asymmetry  $A_{FB}(\hat{s})$ , which is defined as

$$A_{FB}(\hat{s}) = \frac{1}{d\Gamma(B \rightarrow K^* \ell^+ \ell^-)/d\hat{s}} \left[ \int_0^1 d\cos(\theta) \frac{d^2\Gamma(B \rightarrow K^* \ell^+ \ell^-)}{d\hat{s} d\cos(\theta)} - \int_{-1}^0 d\cos(\theta) \frac{d^2\Gamma(B \rightarrow K^* \ell^+ \ell^-)}{d\hat{s} d\cos(\theta)} \right], \quad (38)$$

where  $\theta$  is the angle between the charged lepton  $\ell^+$  and the  $B$ -meson directions in the rest frame of the lepton pair. As is well known, the FB asymmetry is sensitive to the parity structure of the electroweak interaction. At low values of  $q^2$  the parity-conserving photon exchange is expected to dominate and therefore the FB asymmetry should be small; on the contrary, at large  $q^2$  the contribution of the parity-violating  $Z$ - and  $W$ -boson exchanges becomes relevant, leading to a large asymmetry. Moreover, the FB asymmetry is sensitive to the relative sign of the Wilson coefficients [5] and therefore its measurement could be used as a probe of the new physics beyond the Standard Model. Explicitly, one has

$$A_{FB}(\hat{s}) = \frac{3\hat{s}\sqrt{1-4\hat{m}/\hat{s}}\lambda^{1/2}(1, \hat{s}, \hat{r})R_1(q^2)}{\left(1 + \frac{2\hat{m}}{\hat{s}}\right)\beta_V + 12\hat{m}\delta_V}. \quad (39)$$

Finally, we will consider also the longitudinal lepton polarization asymmetry  $P_L(\hat{s})$  defined as

$$P_L(\hat{s}) = \frac{1}{d\Gamma/d\hat{s}} \left[ \frac{d\Gamma(h=-1)}{d\hat{s}} - \frac{d\Gamma(h=+1)}{d\hat{s}} \right], \quad (40)$$

where  $h = +1(-1)$  means right (left) handed charged lepton  $\ell^-$  in the final state. In case of the rare decay  $B \rightarrow K\ell^+ \ell^-$  one has

$$\begin{aligned}
P_L(\hat{s}) &= \frac{2\sqrt{1-4\hat{m}/\hat{s}}\lambda(1, \hat{s}, \hat{r})}{\left(1 + \frac{2\hat{m}}{\hat{s}}\right)\lambda(1, \hat{s}, \hat{r})\beta_P + 12\hat{m}\delta_P} \\
&\quad \text{Re} \left\{ \left[ C_{9V}^{eff}(m_b, q^2) f_+(q^2) + 2(m_b + m_s) C_{7\gamma}(m_b) s(q^2) \right] C_{10A}^* f_+^*(q^2) \right\}, \quad (41)
\end{aligned}$$

whereas for the process  $B \rightarrow K^* \ell^+ \ell^-$  one gets

$$P_L(\hat{s}) = \frac{2\sqrt{1-4\hat{m}/\hat{s}}}{(1+\frac{2\hat{m}}{\hat{s}})\beta_V + 12\hat{m}\delta_V} \left[ 2\lambda(1,\hat{s},\hat{r})\hat{s}R_G(q^2) + \left(2\hat{s} + \frac{(1-\hat{r}-\hat{s})^2}{4\hat{r}}\right)R_F(q^2) + \frac{\lambda^2(1,\hat{s},\hat{r})}{4\hat{r}}R_{H_+}(q^2) - \frac{\lambda(1,\hat{s},\hat{r})}{4\hat{r}}(\hat{s}-1+\hat{r})R_R(q^2) \right] \quad (42)$$

where

$$\begin{aligned} R_G(q^2) &= \text{Re} \left\{ \left[ C_{9V}^{eff}(m_b, q^2) M_B g(q^2) - \frac{2C_{7\gamma}(m_b)}{\hat{s}} \frac{m_b + m_s}{M_B} g_+(q^2) \right] [C_{10A}(m_b) M_B g(q^2)]^* \right\}, \\ R_F(q^2) &= \text{Re} \left\{ \left[ C_{9V}^{eff}(m_b, q^2) \frac{f(q^2)}{M_B} - \frac{2C_{7\gamma}(m_b)}{\hat{s}} \frac{m_b - m_s}{M_B} (1-\hat{r}) B_0(q^2) \right] \left[ C_{10A}(m_b) \frac{f(q^2)}{M_B} \right]^* \right\}, \\ R_{H_+}(q^2) &= \text{Re} \left\{ \left[ C_{9V}^{eff}(m_b, q^2) M_B a_+(q^2) - \frac{2C_{7\gamma}(m_b)}{\hat{s}} \frac{m_b - m_s}{M_B} B_+(q^2) \right] [C_{10A}(m_b) M_B a_+(q^2)]^* \right\}, \\ R_R(q^2) &= \text{Re} \left\{ \left[ C_{9V}^{eff}(m_b, q^2) \frac{f(q^2)}{M_B} - \frac{2C_{7\gamma}(m_b)}{\hat{s}} \frac{m_b - m_s}{M_B} (1-\hat{r}) B_0(q^2) \right] [C_{10A}(m_b) M_B a_+(q^2)]^* \right\} + \\ &\quad \text{Re} \left\{ \left[ C_{9V}^{eff}(m_b, q^2) M_B a_+(q^2) - \frac{2C_{7\gamma}(m_b)}{\hat{s}} \frac{m_b - m_s}{M_B} B_+(q^2) \right] \left[ C_{10A}(m_b) \frac{f(q^2)}{M_B} \right]^* \right\}. \end{aligned} \quad (43)$$

Notice that for a left-handed massless neutrino Eq. (40) yields  $P_L \equiv -1$ . The same result can be obtained also from Eqs. (37,41, 42).

## V. NUMERICAL ANALYSIS

In this section we analyze the decay rates and lepton asymmetries in the Standard Model: the Wilson coefficients at the scale  $\mu \simeq m_b$  are given in Section 2, and the  $B \rightarrow K, K^*$  transition form factors of the dispersion quark model evaluated with the GI-OGE model wave functions are adopted. For the  $B \rightarrow K^*$  transitions we also consider the lattice-constrained parametrizations of the form factors of Ref. [17]. We denote the two sets of predictions as QM and Lat, respectively.

### A. Decay rates and dilepton distributions

First, let us evaluate the  $|V_{ts}|$ . Combining our QM prediction for the  $T_2(0)$  with the CLEO data on  $B \rightarrow K^* \gamma$  [1] we find

$$|V_{ts}| = 0.038 \pm 0.005^{\text{exp}}. \quad (44)$$

A similar analysis with the lattice-constrained parametrization for  $T_2$  [17] yields  $|V_{ts}| = 0.041 \pm 0.005^{\text{th}} \pm 0.005^{\text{exp}}$ .

The predictions for the dilepton distribution in  $B \rightarrow (K, K^*) \ell^+ \ell^-$  decays are reported in Fig. 3, where the non-resonant contributions are also shown separately. The total decay rates turn out to be at least one order of magnitude larger than the non-resonant decay rates. However, the resonant contributions are strongly peaked in narrow regions around their masses, so that outside these regions the resonance influence is almost negligible. This fact allows one to reliably separate the resonant contribution from the non-resonant one, which is mostly interesting as it contains the information on the Wilson coefficients and in principle allows one to measure these coefficients. The resonance phases are chosen in accordance with the analysis of Ref. [6].

Table IV summarizes our predictions for the non-resonant branching ratios. The branching ratios obtained with the QM and Lat sets of the form factors are given in units  $|V_{ts}/0.038|^2$  and  $|V_{ts}/0.041|^2$ , respectively, such that the  $B \rightarrow K^* \gamma$  branching ratio evaluated with  $C_{7\gamma}(\mu = 5 \text{ GeV})$  in each case is normalized to the central CLEO value [1] if this factor is equal to unity.

Note that the transitions  $B \rightarrow K^* \mu^+ \mu^-$  and  $B \rightarrow K^* e^+ e^-$  have different rates, because the amplitude  $B \rightarrow K^* \ell^+ \ell^-$  has a kinematical pole at  $q^2 = 0$ , which makes the corresponding decay rate very sensitive to the lower boundary of the phase space volume ( $q^2 = 4m_\ell^2$ ), while the amplitude  $B \rightarrow K \ell^+ \ell^-$  is regular at  $q^2 = 0$  and, therefore, insensitive to the mass of the light lepton.

One observes a strong sensitivity of the differential decay rates in  $B \rightarrow K^*$  transitions at low  $q^2$ : the decay rates are results of the interference of various form factors and thus are sensitive to the details of their  $q^2$ -behavior. One can see that the Lat and QM form factor sets which both provide a reasonable agreement with the lattice results at large  $q^2$ , yield sizeable deviations in the differential distributions at low  $q^2$  and hence in the

branching ratios. Thus for deriving accurate predictions for the branching ratios one needs accurate knowledge of the form factors at low  $q^2$ .

The decay rates of the  $B \rightarrow K$  modes turn out to be more stable with respect to variations of the relevant form factors (cf. [11]) and thus might be more perspective for extracting  $V_{ts}$  from rare semileptonic decays.

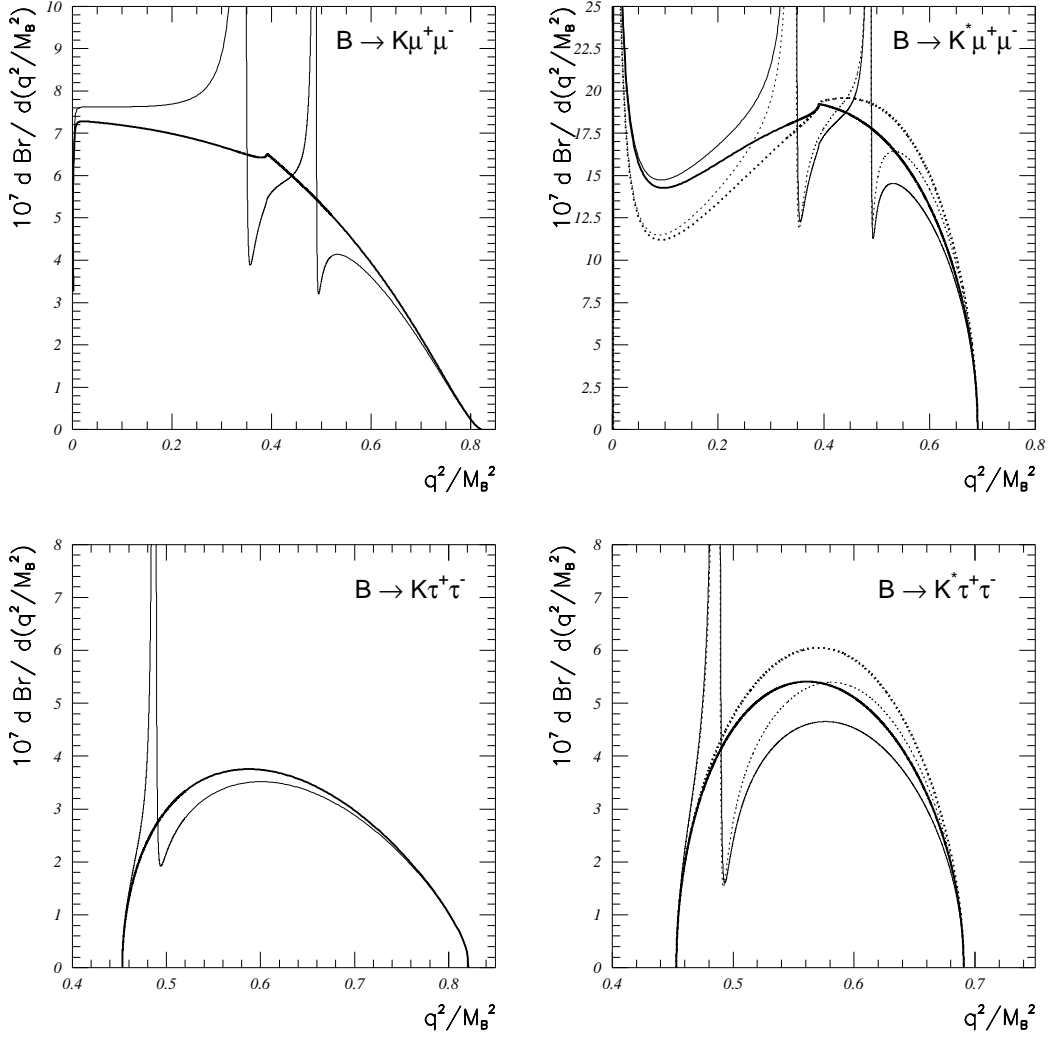


FIG. 3. Differential decay rates  $10^7 d Br/d(q^2/M_B^2)$  in the decays  $B \rightarrow K^* \ell^+ \ell^-$ : a.  $B \rightarrow K \mu^+ \mu^-$ . b.  $B \rightarrow K^* \mu^+ \mu^-$ . c.  $B \rightarrow K \tau^+ \tau^-$ , d.  $B \rightarrow K^* \tau^+ \tau^-$ . Solid - QM form factors (GI-OGE), for  $|V_{ts}| = 0.038$ ; dotted - lattice-constrained parametrization of [17], for  $|V_{ts}| = 0.041$ . Thick lines - nonresonant parts, thin lines - total.

TABLE IV. Non-resonant branching fractions of the radiative and rare semileptonic  $B$  decays. The branching fractions are evaluated using  $\mathcal{H}_{eff}$  at the scale  $\mu = 5$  GeV. Uncertainties connected with a relevant choice of this low-energy scale  $\mu \sim m_b$  are not shown.

Decay mode	QM $\times  V_{ts}/0.038 ^2$	Lat $\times  V_{ts}/0.041 ^2$	[5] $\times  V_{ts}/0.033 ^2$	Exp.
$B \rightarrow K^* \gamma$	$4.2 \times 10^{-5}$	$4.2 \times 10^{-5}$	$(4.9 \pm 2.0) \times 10^{-5}$	$(4.2 \pm 1.0) \times 10^{-5}$ [1]
$B \rightarrow K^* e^+ e^-$	$1.50 \times 10^{-6}$	$1.45 \times 10^{-6}$	$(2.3 \pm 0.9) \times 10^{-6}$	$< 1.6 \times 10^{-5}$ [32]
$B \rightarrow K^* \mu^+ \mu^-$	$1.15 \times 10^{-6}$	$1.1 \times 10^{-6}$	$(1.5 \pm 0.6) \times 10^{-6}$	$< 2.5 \times 10^{-5}$ [33]
$B \rightarrow K^* \tau^+ \tau^-$	$1.0 \times 10^{-7}$	$1.1 \times 10^{-7}$	—	—
$B \rightarrow K^* \sum \nu_i \bar{\nu}_i$	$1.5 \times 10^{-5}$	$1.4 \times 10^{-5}$	$(1.1 \pm 0.55) \times 10^{-5}$	—
$B \rightarrow K \ell^+ \ell^-$	$4.4 \times 10^{-7}$	—	$(4.0 \pm 1.5) \times 10^{-7}$	$< 0.9 \times 10^{-5}$ [32]
$B \rightarrow K \tau^+ \tau^-$	$1.0 \times 10^{-7}$	—	—	—
$B \rightarrow K \sum \nu_i \bar{\nu}_i$	$5.6 \times 10^{-6}$	—	$(3.2 \pm 1.6) \times 10^{-6}$	—

## B. Forward-backward asymmetry

The forward-backward dilepton asymmetries in  $B \rightarrow K^* \ell^+ \ell^-$  decays are presented in Fig. 4. For comparison, we show also nonresonant  $A_{FB}$  evaluated with the form factors for the ISGW2 quark model parameters, and obtained assuming the HQS relations between the form factors. One can observe a strong sensitivity of the asymmetries to the specific details of the behavior of the relevant form factors. Notice that the maximum of the asymmetry at  $q^2/M_B^2 \simeq 0.1$  is mainly proportional to the ratio  $(V/A_1)^2$ . That is why the Lat  $A_{FB}$  turns out to be larger in the maximum than the QM asymmetry. Nevertheless the general trend of the behavior of  $A_{FB}$  for all considered sets of the form factors is similar: the nonresonant asymmetry is positive at low  $q^2$ , has a zero at  $q^2/M_B^2 \simeq 0.15$ , and then becomes negative irrespective to the details of the form factor behavior. Let us point out that maximum absolute value of the (negative) asymmetry is attained at  $q^2/M_B^2 \simeq 0.62$  where  $|A_{FB}| \simeq 0.4$  both for the QM and Lat sets of the form factors. This is considerably smaller than  $|A_{FB}| \simeq 0.6$  reported in [12]. This difference is traced back to a very specific behavior of the form factor  $T_3$  in [12] which contradicts to the results of other approaches and to the approximate HQS relations between the form factors (see also discussion in [11]).

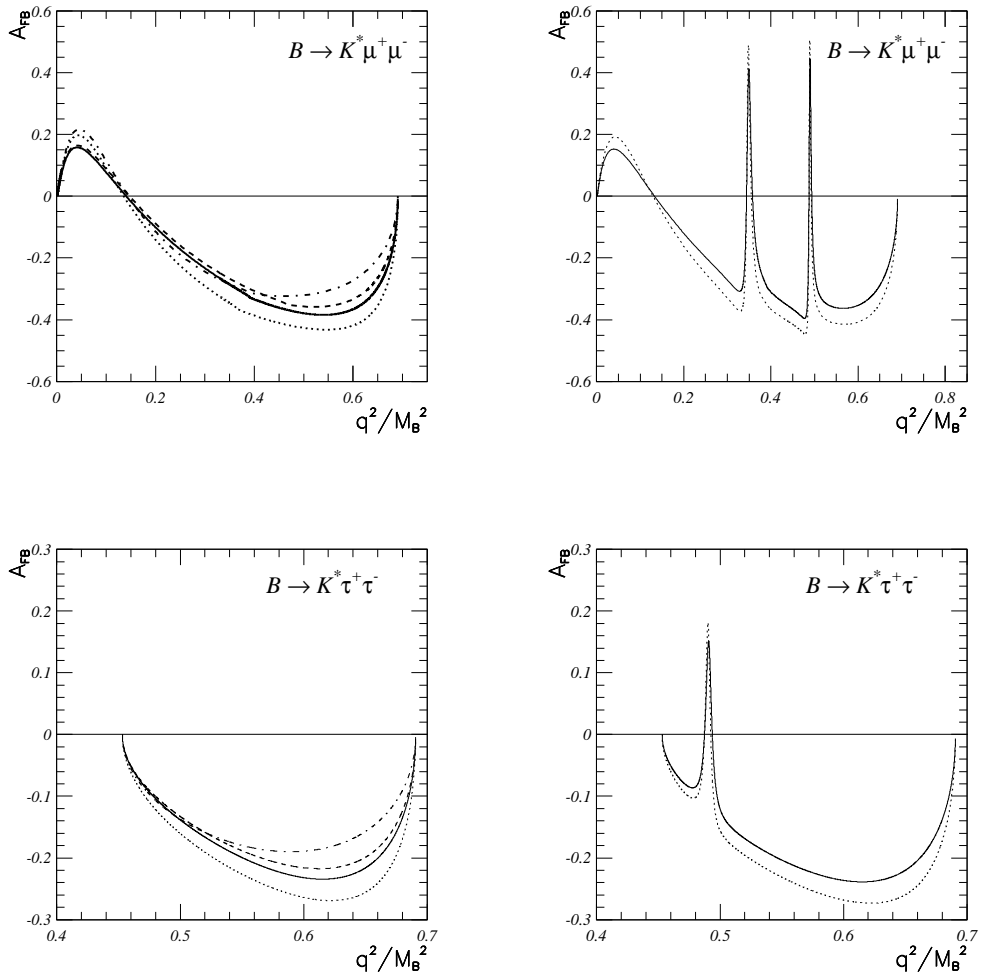


FIG. 4. Forward-backward asymmetries in  $B \rightarrow K^* \ell^+ \ell^-$  transitions. a.  $B \rightarrow K^* \mu^+ \mu^- (e^+ e^-)$ , non-resonant. b. The same, total. c.  $B \rightarrow K^* \tau^+ \tau^-$ , non-resonant. d. The same, total. Solid - GI-OGE, dashed - ISGW2 models, dotted - lattice-constrained parametrization of [17], dash-dotted - HQS relations.

### C. Lepton polarization asymmetry

Fig. 5 shows lepton polarization asymmetries  $P_L$  for massless and massive leptons. For understanding the behavior of  $P_L$  it is important to take into account the relationship between the Wilson coefficients in the SM:

$$C_{7\gamma}(m_b) \ll C_{10A}(m_b) \simeq -C_{9V}(m_b). \quad (45)$$

In the case of the transition  $B \rightarrow K\ell^+\ell^-$ ,  $\ell = \mu, e$  a simple analysis of Eq. (41) yields the following behavior of the nonresonant  $P_L$ :  $P_L$  is equal to zero at  $q^2 = 4m_\ell^2$  and  $q^2 = (M_b - M_K)^2$  due to kinematical reasons, and in the intermediate region of  $q^2$ ,  $P_L$  steeply goes down to the value  $P_L \simeq 2C_{9V}C_{10A}/(C_{9V}^2 + C_{10A}^2) \simeq -1$  independently of the particular behavior of the  $B \rightarrow K$  transition form factors. A weak  $q^2$ -dependence of the nonresonance  $P_L$  is due to the function  $h(m_c/m_b, q^2/m_b^2)$  in  $C_{9V}^{eff}$ .

In the reaction  $B \rightarrow K^*\ell^+\ell^-$ ,  $\ell = \mu, e$  the situation is a bit different: Now the term in  $\mathcal{H}_{eff}$  proportional to a small  $C_{7\gamma}$  contains a photon pole at  $q^2 = 0$  and thus a parity-conserving photon exchange dominates the decay at low  $q^2$  providing a small value of  $P_L$ . At large  $q^2$  one finds  $P_L \simeq -1$  because of just the same reason as in the  $B \rightarrow K$  case with the only difference is that the kinematical zero at  $q^2 = (M_B - M_{K^*})^2$  is absent. In the intermediate region of  $q^2$ , the nonresonant  $P_L$  is an interplay of the parity-conserving and parity-violating terms yielding a negative  $P_L$  smoothly falling from 0 to  $-1$  in a way largely independent of the particular  $q^2$ -dependence of the transition form factors.

In the total  $P_L$  in the reactions  $B \rightarrow (K, K^*)\ell^+\ell^-$ ,  $\ell = \mu, e$  the  $\psi$  and  $\psi'$  resonances appear as sharp peaks on a smooth nonresonance background.

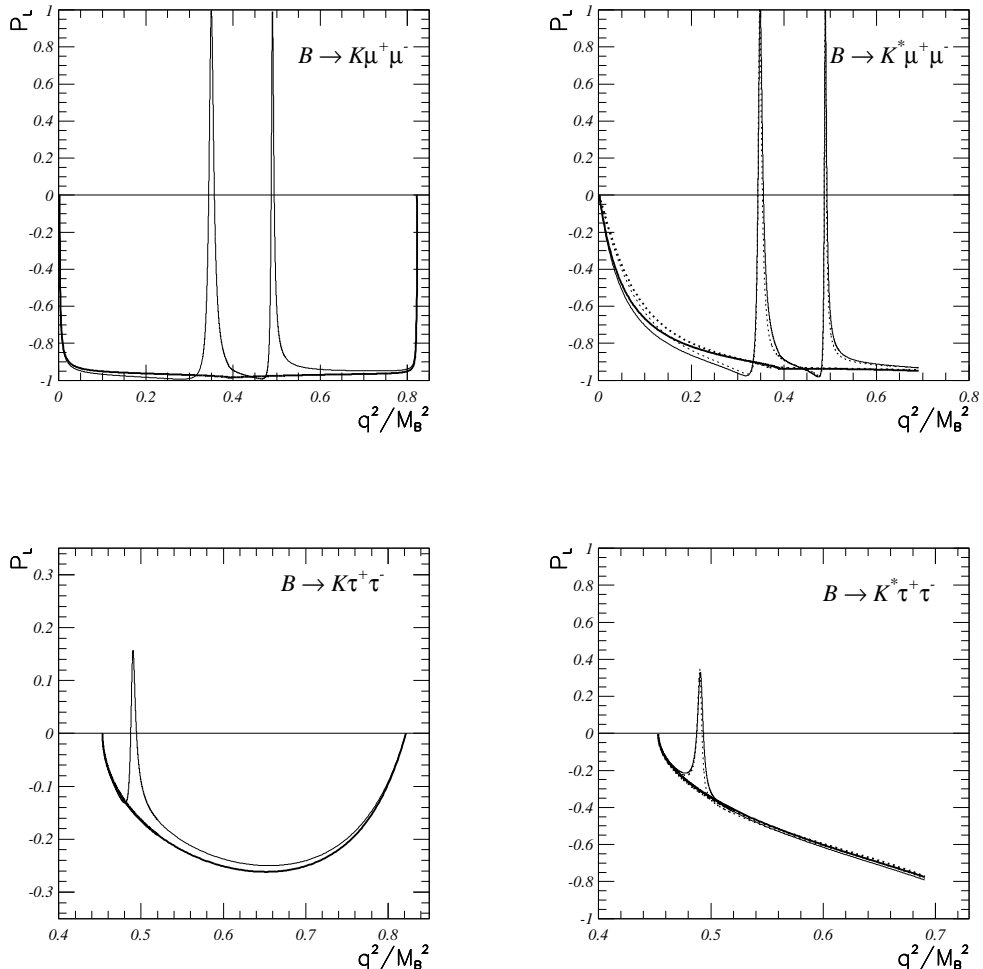


FIG. 5. Longitudinal lepton polarization asymmetry ( $P_L$ ) in the decays  $B \rightarrow (K, K^*)\ell^+\ell^-$ : a.  $B \rightarrow K\mu^+\mu^-(e^+e^-)$ . b.  $B \rightarrow K^*\mu^+\mu^-(e^+e^-)$ . c.  $B \rightarrow K\tau^+\tau^-$ . d.  $B \rightarrow K^*\tau^+\tau^-$ . Solid - GI-OGE, dotted - lattice-constrained parametrization of [17]. Thick lines - nonresonant, thin lines - total.

The results of our calculation shown in Fig. 5 as well as the results of Ref. [10,11] correspond to the picture described above, whereas  $P_L$  reported in [13] has a different behavior with  $P_L \simeq -0.6$  at large  $q^2$  which seems to be very doubtful.

The lepton polarization asymmetry  $P_L$  in the case  $B \rightarrow (K, K^*)\tau^+\tau^-$  in general follows the trend of the light leptons case with an important difference: the nonresonant  $P_L$  does not go down to the value  $\simeq -1$  in the kinematically accessible region. The  $P_L$  again turns out to be largely insensitive to the meson transition form factors. In the total  $P_L$  one observes only the  $\psi'$  peak in the kinematically accessible region.

## VI. CONCLUSIONS

We have analyzed rare semileptonic transitions  $B \rightarrow (K, K^*)$  within the Standard Model adopting two models for the relevant form factors: a relativistic constituent quark model, formulated in a dispersion form, and the lattice-constrained parametrization of Ref. [17]. Our main results are as follows:

- We have presented a dispersion quark model calculation of the  $B \rightarrow K, K^*$  transition form factors in the whole kinematical range of  $q^2$ . Adopting the quark masses and the wave functions of the Godfrey-Isgur model [28] for the hadron spectrum with a switched-off one-gluon exchange potential for taking into account only the impact of the confinement scale, we have found the resulting form factors to be in good agreement with the lattice simulations at large  $q^2$ .

The form factors in the dispersion quark model develop the correct expansion in the leading and next-to-leading  $1/m_Q$  orders for the heavy-to-heavy decays, and satisfy the relations between the form factors of the vector, axial-vector, and tensor currents valid in the region near the zero-recoil point in case of heavy-to-light decays. In addition, the form factors are compatible with known analytical constraints.

Hence, the form factors of the dispersion quark model obey all existing rigorous theoretical constraints and agree nicely with the results of lattice simulations for the  $B \rightarrow K^*$  decay at large  $q^2$ . Moreover, the dispersion quark model form factors for the  $B \rightarrow K^*$  transition agree favorably in the whole range of  $0 < q^2 < (M_B - M_K^*)^2$  with a lattice-constrained fit [17] based on the constituent quark picture [9] and an assumption on a single-pole behavior of  $A_1(q^2)$ . Thus we expect to have reliable form factors in the whole kinematically accessible decay region.

- We have performed a detailed analysis of the non-resonant decay rates and asymmetries in  $B \rightarrow (K, K^*) (\ell^+\ell^-, \nu\bar{\nu})$  decays in the Standard Model and obtained predictions for all exclusive channels using our GI-OGE form factors and the lattice-constrained fit to the form factors of  $B \rightarrow K^*$  transition.

i. Combining our QM result for  $T_2(0)$  with the central CLEO value for  $B \rightarrow K^*\gamma$  [1] we estimate the central value  $|V_{ts}| = 0.038$ . With the lattice-constrained parametrization of the form factors [17] one finds the central value  $|V_{ts}| = 0.041$ .

ii. The results of the non-resonant branching fractions, obtained within the two sets of the form factors, are in good agreement if the relevant  $|V_{ts}|$  is used in each case. Nevertheless, a better knowledge of the relevant form factors around  $q^2 = 0$  is still required.

iii. The differential dilepton distributions in  $B \rightarrow K\ell^+\ell^-$  decays are less sensitive to the details of  $q^2$ -behavior of the form factors than the corresponding distributions in  $B \rightarrow K^*\ell^+\ell^-$  processes. Thus, the reaction  $B \rightarrow K\mu^+\mu^-$  seems to be the most appropriate one for the determination of  $V_{ts}$  from rare exclusive semileptonic decays.

iv. The shape of the forward-backward asymmetry in  $B \rightarrow K^*\mu^+\mu^-$  within the SM is almost independent of the long-distance contributions:  $A_{FB}$  is positive at small  $q^2$ , has a zero at  $q^2 \simeq 0.15M_B^2$  and then becomes negative at larger  $q^2$ . On the other hand, the values of  $A_{FB}$  in the maximum and the minimum are determined by the ratios of the form factors (see also discussion in [34]).

v. The longitudinal lepton polarization asymmetry  $P_L(B \rightarrow K\mu^+\mu^-)$  at all kinematically accessible  $q^2$ , except for the end-points and narrow regions near  $\psi$  and  $\psi'$ , as well as  $P_L(B \rightarrow K^*\mu^+\mu^-)$  at large  $q^2$  do not depend on the long-distance contributions. In particular,  $P_L(B \rightarrow K\mu^+\mu^-) \simeq 2C_{9V}C_{10A}/(C_{9V}^2 + C_{10A}^2) (\simeq -1$  in the SM), and hence  $P_L$  directly measures the ratio of the Wilson coefficients  $C_{9V}/C_{10A}$  at the scale  $\mu \simeq m_b$ . Thus, the experimental study of the forward-backward asymmetry and the longitudinal lepton polarization asymmetry provides an effective test of the Standard Model and its possible extinctions.

The presented results for the decay rates are essentially based on the lattice-constrained constituent quark picture. Further progress in obtaining more accurate predictions by combining these approaches may be expected on the following way: with increasing the accuracy of the lattice predictions one can put forward the determination of the meson wave functions from the least- $\chi^2$  fit to the lattice results at small recoils, basing on

our proposed spectral representations for the form factors. Then such lattice-constrained quark model would provide reliable and accurate form factors at all kinematically accessible  $q^2$ .

## VII. ACKNOWLEDGMENTS

We are grateful to D. Becirevic, V. Braun, A. Le Yaouanc, and B. Stech for helpful discussions. The work was supported in part by RFBR grants 95-02-04808a and 96-02-18121a.

---

[1] R. Ammar *et al.*, Phys. Rev. Lett. **71**, 674 (1993) and CLEO CONF 96-05 (1996).  
[2] M. S. Alam *et al.*: Phys. Rev. Lett. **74**, 2885 (1995).  
[3] B. Grinstein, M. B. Wise and M. J. Savage, Nucl. Phys. B **319**, 271 (1989).  
[4] A. Buras and M. Münz, Phys. Rev. D **52**, 186 (1995).  
[5] A. Ali, T. Mannel and T. Morozumi, Phys. Lett. B **273**, 505 (1991);  
A. Ali, Acta Phys. Pol. B **27**, 3529 (1996); Nucl. Instrum. Meth. A **384**, 8 (1996).  
[6] C. S. Lim, T. Morozumi and A. T. Sanda, Phys. Lett. B **218**, 343 (1989);  
P. J. O'Donnell and H. K. K. Tung, Phys. Rev. D **43**, R2067 (1991).  
[7] T. Inami and C. S. Lim: Prog. Theor. Phys. **65**, 287 (1981); G. Buchalla and A. J. Buras, Nucl. Phys. B **400**, 225 (1993).  
[8] W. Jaus and D. Wyler, Phys. Rev. D **41**, 3405 (1990).  
[9] B. Stech, Phys. Lett. B **354**, 447 (1995); Z. Phys. C **75**, 245 (1997).  
[10] C. Q. Geng and C. P. Kao, Phys. Rev. D **54**, 5636 (1996).  
[11] D. Melikhov, N. Nikitin, S. Simula, Phys. Lett. B **410**, 290 (1997).  
[12] P. Colangelo *et al.*, Phys. Rev. D **53**, 3672 (1996); Phys. Lett. B **395**, 339 (1997).  
[13] T. M. Aliev *et al.*, Phys. Rev. D **56**, 4260 (1997); Phys. Lett. B **400**, 194 (1997).  
[14] D. Becirevic, e-print archive hep-ph/9707271.  
[15] APE Collaboration, A. Abada *et al.*, Phys. Lett. B **365**, 275 (1996).  
[16] UKQCD Collaboration, J. M. Flynn and C. T. Sachrajda, e-print archive hep-lat/9710057;  
J. M. Flynn *et al.*, Nucl. Phys. B **461**, 327 (1996);  
[17] UKQCD Collaboration, L. Del Debbio *et al.*, e-print archive hep-lat/9708008 (1997).  
[18] G. Burdman, Phys. Rev. D **52**, 6400 (1995); W. Roberts, Phys. Rev. D **54**, 863 (1996).  
[19] L. Lellouch, Nucl. Phys. B **479** (1996) 353.  
[20] P. Ball and V. M. Braun, Phys. Rev. D **55**, 5561 (1997).  
[21] D. Melikhov, Phys. Rev. D **53**, 2460 (1996); Phys. Lett. B **380**, 363 (1996); Phys. Lett. B **394**, 385 (1997).  
[22] D. Melikhov, e-print archive hep-ph/9706417, to be published in Phys. Rev. D **56** (1997).  
[23] N. Isgur and M. B. Wise, Phys. Lett. B **232**, 113 (1989); Phys. Lett. B **237**, 527 (1990);  
[24] M. Luke, Phys. Lett. B **252**, 447 (1990); M. Neubert and V. Rieckert, Nucl. Phys. B **382**, 97 (1992).  
[25] N. Isgur and M. B. Wise, Phys. Rev. D **42**, 2388 (1990).  
[26] D. Scora and N. Isgur, Phys. Rev. D **52**, 2783 (1995).  
[27] F. Cardarelli *et al.*, Phys. Lett. B **332**, 1 (1994); Phys. Lett. B **349**, 393 (1995); Phys. Lett. B **359**, 1 (1995);  
Few-Body Syst. Suppl. **9**, 267 (1995); Phys. Rev. D **53**, 6682 (1996).  
[28] S. Godfrey and N. Isgur, Phys. Rev. D **32**, 189 (1985).  
[29] I. L. Grach, I. M. Narodetskii and S. Simula, Phys. Lett. **B385**, 317 (1996);  
N. B. Demchuk, I. L. Grach, I. M. Narodetskii and S. Simula, Phys. Atom. Nucl. **59**, 2152 (1996).  
[30] S. Simula, Phys. Lett. B **373**, 193 (1996).  
[31] F. Krüger and L. M. Sehgal, Phys. Rev. D **56**, 5452 (1997).  
[32] T. Skwarnicki, in *Proc. of the 17<sup>th</sup> Int. Symp. on Lepton-Photon Interactions*, Beijing (China), August 1995, eds.  
Z. Zhi-Peng and C. He-Sheng (World Scientific), p. 238.  
[33] C. Anway-Wiese *et al.*, FERMILAB CONF-95-201-E (1995); T. Speer *et al.*; FERMILAB CONF-96-320-E (1996).  
[34] D. Melikhov, *Talk given at 32-nd Rencontres de Moriond: Electroweak Interactions and Unified Theories*, Les Arcs, France, 15-22, Mar 1997 (e-print archive hep-ph/9704421); G. Burdman, e-print archive hep-ph/9710550.